ACADEMIC PRESS

Available online at www.sciencedirect.com

SCIENCE DIRECT®

Journal of Sound and Vibration 262 (2003) 87–115

JOURNAL OF SOUND AND VIBRATION

www.elsevier.com/locate/jsvi

Basic sound generation mechanisms in inviscid vortex interactions at low Mach number

S.K. Tang[a,*], N.W.M. Ko[b]

[a] *Department of Building Services Engineering, The Hong Kong Polytechnic University, Hong Kong, People's Republic of China*

[b] *Department of Mechanical Engineering, The University of Hong Kong, Hong Kong, People's Republic of China*

Received 19 July 2001; accepted 17 June 2002

Abstract

The sound generation mechanisms during finite core vortex interactions at low Mach number are investigated in the present study. The theoretical deductions show clearly that the basic sound generation mechanisms are associated with the vortex core deformation and the vorticity centroid dynamics, independent of the vortex system. Such deductions are substantiated by numerical experiments with the interactions of two-dimensional vortices, vortex pairs and vortex rings. Detailed discussions on the similarities and differences between the sound generation processes of the two-dimensional and axisymmetric vortex systems are given. The relative importance of the two sound generation mechanisms in these vortex systems, their characteristics and interactions, which are hardly found in existing literature, are also examined. The present findings have also generalized and substantiated the previous results of the authors on the topic.

1. Introduction

The turbulence generated by shear flows is sound producing. Since Lighthill [1] proposed the aeroacoustic model using the stress tensor as the source, many models of turbulence sound generation have been developed. Typical examples include the vortex sound theory of Powell [2], the instability wave model of Ffowcs Williams and Kempton [3] and the stagnation enthalpy of Doak [4].

The topic has also been studied through direct numerical simulation. The results of Colonius et al. [5] and Mitchell et al. [6] pointed out that the conventional acoustical analogy gives rise to

*Corresponding author. Tel.: +852-2766-7782; fax: +852-2774-6146.
E-mail address: besktang@polyu.edu.hk (S.K. Tang).

0022-460X/03/$ - see front matter
doi:10.1016/S0022-460X(02)01029-5

source terms that may not have direct contribution to the overall sound field produced by a shear layer. Their results show some features of the experimentally measured sound field. The source terms they specified are related to the local fluid velocities and their gradients. Freund [7], in a recent direct numerical simulation study, computed the Lighthill's source using Fourier methods for a low-Reynolds-number transonic turbulent jet and demonstrated that the results so obtained agreed to a great extent with the experiment.

The vortices have attracted the attention of many researchers, due to their simplicity and the inherited difficulties in handling turbulence. Küchemann [8] has concluded the importance of vortices in the study of turbulent shear flows. The theory of vortex sound shows explicitly the importance of unsteady vortex motion on the production of sound [3]. Knio et al. [9] investigated the sound produced by the interactions between two-dimensional vortices using basically acoustic analogy with Möhring's source term [10]. They suggested the importance of vortex core motions and vortex core perturbations on the production of sound. Möhring [11] has also discussed the importance of vortex ring centroidal motions on sound generation. However, the relative importance of various sound generation mechanisms, their interactions and characteristics in the interacting finite core vortex systems are not explicitly addressed. Howe [12] and also Möhring [11] investigated the sound produced by unsteady two-dimensional elliptic core vortex motions, but they dealt with time-invariant core shapes, which may be a drastic simplification for finite core vortex interactions in which the cores are not elliptical and their shapes are functions of time [13].

The numerical results of Leung et al. [14] show that the pairing of two thin inviscid vortex rings can produce a sound field having the essential characteristics of jet noise. The results of the numerical studies of the authors [13,15,16], using the method of contour dynamics, have illustrated the importance of vortex acceleration and jerk in the production of sound by the interactions of two finite core vortices. These findings appear consistent with the experimental results of Tang and Ko [17], which, to the authors' knowledge, reported the first direct comparison between theory and experiment in the study of sound generation by unsteady motions of the vortical structures in an air jet.

More recent numerical results of the authors on the low-Mach-number sound generation by the interaction of two vortex pairs [18] suggest that the sound source term can be separated into two components: one component is related to the vortex centroid dynamics and the other to the microscopic vortex core deformation. Their results also suggest a possible generalization of sound sources in the interactions between two inviscid finite core vortices at low Mach number. This recent work [18] discussed the characteristics of various sources and has provided a physical interpretation of the sound generation process involving coherent structures inside turbulent shear flows. Though the vortex centroid dynamics and the vortex core deformation may not be easily measured experimentally, they can be studied using the direct numerical simulation method. A carefully designed conditional sampling experiment [19] can help their recovery.

This paper is an attempt to extend the work of Tang and Ko [18] to different vortex interaction systems, such that the basic sound generation mechanisms can be established. Sound production by the leapfrogging motions, coalescence and collisions between two vortex rings, two vortex pairs and two two-dimensional vortices (without collision) will be studied and presented. It is also aimed at examining the similarities and differences in the mechanisms of sound generation in the two-dimensional and axisymmetric vortex systems. The importance of and the interactions

between different sound generation mechanisms in the overall sound generation processes will be discussed.

2. Theoretical considerations

2.1. Method of contour dynamics

This method was first developed by Zabusky et al. [20] for the calculations of non-linear vortex patch evolution. Each vortex core boundary is treated as a contour. The velocity of each element on these boundaries is calculated by using the Biot–Savart induction law in the presence of vorticity. One can observe that the fluid velocity, $\boldsymbol{u}$, at a point, $\boldsymbol{y}$, in the flow field (near field) is related to the local streamfunction ψ as

$$\boldsymbol{u} = \nabla \times (\psi f(\boldsymbol{y})), \tag{1}$$

where $f(\boldsymbol{y})$ is a vector function depending on the vortex system. The vorticity transport equation for an incompressible flow suggests

$$\frac{D}{Dt}(\omega |f(\boldsymbol{y})|) = 0, \tag{2}$$

where t is the interaction time and ω the vorticity at the point $\boldsymbol{y}$. Eqs. (1) and (2) can be solved once the system Green function are known [20,21]. The calculation of $\boldsymbol{u}$ involves an integration over the cross-sections of the vortex cores, which can be transformed into a contour integral using the Stoke's theorem. Full details on the application of this method in the two-dimensional and axisymmetrical vortex systems can be found, for example in Zabusky et al. [20] and Pozrikidis [21], respectively, and are not repeated in the present paper. Some simplified version of the theory can also be found in the previous works of the authors [16].

In order to ensure smooth vortex boundaries and efficient computations throughout the numerical experiment, the node point insertion and relaxation procedure employed by Pozrikidis and Higdon [22] were adopted. All the contour integrals involved were computed using the four-point Gaussian quadrature procedure. The vortex core shapes were obtained by integrating the core boundary velocities with respect to time, using the fourth order Runge–Kutta method.

2.2. Vortex sound generation mechanisms

According to theory of Howe [12], the acoustic variable in the full equation for aeroacoustics is the stagnation enthalpy. The sources are related to vortex motions and flow entropy. However, in the low-Mach-number inviscid condition, his theory reduces to that of Powell [2]. The farfield pressure fluctuations, p, generated by the low-Mach-number unsteady motions of vorticity-bearing fluids can be obtained by solving the following inhomogeneous equation:

$$\frac{1}{c^2}\frac{\partial^2 p}{\partial \tau^2} - \nabla^2 p = \rho_0 \nabla \cdot (\omega \times \boldsymbol{u}), \tag{3}$$

where c and ρ_0 are the speed of sound in and the density of the ambient fluid respectively. The general solution of Eq. (3) for p at a farfield displacement $\boldsymbol{x}$ depends on the type of vortex system

concerned. In the present study, it is assumed that the farfield distance $|\boldsymbol{x}|$ is much greater than any length scale in the vortex system cross-section. The theory of Möhring [10,11] is used in the present study. However, Crow [23] has pointed out that acoustic analogy is asymptotically incorrect for any flow where the total vortical region is substantially larger than any particular eddy in the flow, that is, when the flow/acoustic interactions become important. The present use of the acoustic analogy is therefore restricted to those cases when flow/acoustic interactions may be neglected.

2.2.1. Two-dimensional vortex system

Both the two-dimensional vortices [13] and the vortex pairs [18] belong to this category and they produce non-compact flow fields. Their motions and the positions of their boundaries can be described by using the longitudinal and transverse co-ordinates, denoted as y_1 and y_2, respectively (Fig. 1). The spanwise direction y_3 is important only in the evaluation of the final farfield pressure fluctuations as the integral in Eq. (4) has to be taken over this length scale from $-\infty$ to $+\infty$ [13]. In this vortex system, $f(\boldsymbol{y})$ in Eq. (1) equals $\hat{y}_3$.

Let A be the cross-sectional area of the vortex system which extends to infinite in the y_3 direction, the farfield pressure fluctuation p can be expressed as, following the results of Möhring [11],

$$p(\boldsymbol{x},\tau)=\frac{\rho_0}{8\pi c^2}\int_{-\infty}^{\infty}\frac{1}{|\boldsymbol{x}-\boldsymbol{y}|}\frac{\partial^3}{\partial t^3}\left(\cos 2\theta\oint\omega y_1 y_2\,\mathrm{d}A+\sin 2\theta\oint\frac{y_2^2-y_1^2}{2}\omega\,\mathrm{d}A\right)\mathrm{d}y_3, \tag{4}$$

where the differentiation is taken at the retarded time $\tau-|\boldsymbol{x}-\boldsymbol{y}|/c$. There are two quadrupoles co-existing. The integration over y_3 is not performed in the present study as it has no bearing on the sound generation mechanism. One should note that Eq. (4) is equivalent to the formula derived by Möhring [11]. Details on this equivalence are given in the appendix. A Fourier transform of Eq. (4) with respect to τ gives the formula used by Knio et al. [9] provided that $|\boldsymbol{x}|\to\infty$. Two source terms are thus identified

$$S_1=\oint\omega y_1 y_2\,\mathrm{d}A\quad\text{and}\quad S_2=\frac{1}{2}\oint(y_2^2-y_1^2)\omega\,\mathrm{d}A. \tag{5}$$

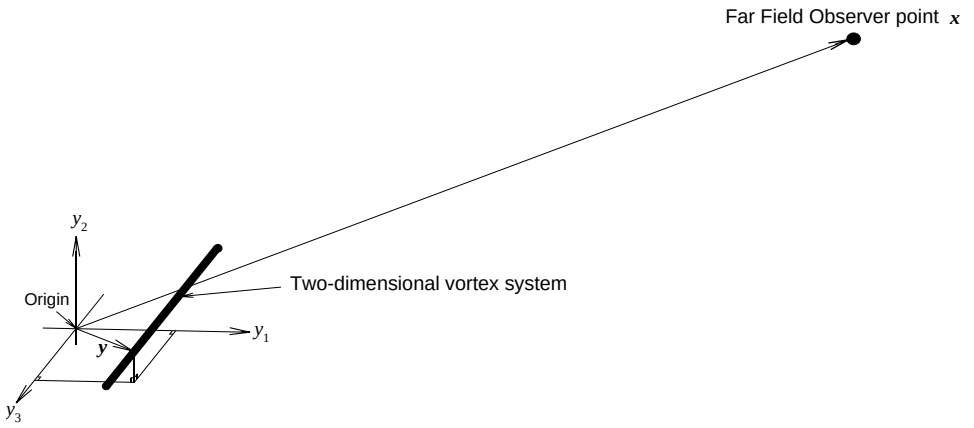

Fig. 1. Schematic diagram for two-dimensional vortex system.

Since the steady motion of vorticity is not a source of sound, the effects of any mean motions in these two source terms have to be eliminated so that the discussions will not be affected by these mean terms, all of which are not contributing to the final sound field. To do this, one defines the vorticity centroid of the whole vortex system $\boldsymbol{y}_{sc}$ as

$$\boldsymbol{y}_{sc} = \oint \omega \boldsymbol{y}\, \mathrm{d}A / \oint \omega\, \mathrm{d}A = y_{sc1}\hat{y}_1 + y_{sc2}\hat{y}_2. \tag{6}$$

Then, the position of a point inside the vortex core $\boldsymbol{y}'$ relative to the mean motion can be written as $\boldsymbol{y}' = \boldsymbol{y} - \boldsymbol{y}_{sc}$. Thus,

$$S_1 = \oint \omega y_1 y_2\, \mathrm{d}A = \oint \omega y_1' y_2'\, \mathrm{d}A + y_{sc1} \oint \omega y_2'\, \mathrm{d}A + y_{sc2} \oint \omega y_1'\, \mathrm{d}A + y_{sc1} y_{sc2} \oint \omega\, \mathrm{d}A \tag{7a}$$

and

$$S_2 = \frac{1}{2} \oint \omega(y_2'^2 - y_1'^2)\, \mathrm{d}A + y_{sc2} \oint \omega y_2'\, \mathrm{d}A - y_{sc1} \oint \omega y_1'\, \mathrm{d}A + \frac{y_{sc2}^2 - y_{sc1}^2}{2} \oint \omega\, \mathrm{d}A. \tag{7b}$$

One can observe that the integral $\oint \omega y_i'\, \mathrm{d}A$ $(i = 1, 2)$ either vanishes or is a constant, due to the conservation of vortex impulse. $\oint \omega\, \mathrm{d}A$ is the total circulation and is again a constant. The source strengths of the two quadrupoles are

$$\frac{\partial^3 S_1}{\partial t^3} = \frac{\partial^3}{\partial t^3} \oint \omega y_1' y_2'\, \mathrm{d}A + \oint \omega y_1'\, \mathrm{d}A \frac{\partial^3 y_{sc2}}{\partial t^3} + \oint \omega y_2'\, \mathrm{d}A \frac{\partial^3 y_{sc1}}{\partial t^3} + \oint \omega\, \mathrm{d}A \frac{\partial^3 y_{sc1} y_{sc2}}{\partial t^3} \tag{8a}$$

and

$$\begin{aligned} \frac{\partial^3 S_2}{\partial t^3} = & \frac{\partial^3}{\partial t^3} \oint \left(\frac{y_2'^2 - y_1'^2}{2} \right) \omega\, \mathrm{d}A + \oint \omega y_2'\, \mathrm{d}A \frac{\partial^3 y_{sc2}}{\partial t^3} - \oint \omega y_1'\, \mathrm{d}A \frac{\partial^3 y_{sc1}}{\partial t^3} \\ & + \oint \omega\, \mathrm{d}A \frac{\partial^3}{\partial t^3} \left(\frac{y_{sc2}^2 - y_{sc1}^2}{2} \right). \end{aligned} \tag{8b}$$

The quantities involved in Eq. (8) are all Galilean invariants. Eq. (8) suggests the importance of the system vorticity centroid unsteady motions and the system impulse in the production of sound. However, not all of them are significant in symmetrical systems, such as the two-dimensional vortices and vortex pairs. This will be discussed later.

Focusing on one of the interacting vortices and further defining $\boldsymbol{y}'' = \boldsymbol{y}' - \boldsymbol{y}_c$, where $\boldsymbol{y}_c$ denotes the vorticity centroid of the vortex concerned relative to the system vorticity centroid motion, it can be shown that

$$\oint \omega y_1' y_2'\, \mathrm{d}A = \oint \omega y_1'' y_2''\, \mathrm{d}A + y_{c1} \oint \omega y_2''\, \mathrm{d}A + y_{c2} \oint \omega y_1''\, \mathrm{d}A + y_{c1} y_{c2} \oint \omega\, \mathrm{d}A \tag{9a}$$

and

$$\frac{1}{2} \oint \omega(y_2'^2 - y_1'^2)\, \mathrm{d}A = \frac{1}{2} \oint \omega(y_2 - y_1)\, \mathrm{d}A + \sum_{i=1}^{2} (-1)^i y_{ci} \oint \omega y_i''\, \mathrm{d}A + \frac{y_{c2}^2 - y_{c1}^2}{2} \oint \omega\, \mathrm{d}A, \tag{9b}$$

where the integrals are taken over the core of the vortex concerned. Since $\oint \omega y_i''\, \mathrm{d}A \equiv 0$, it follows that there are two main mechanisms through which vortex sound is generated. The first one is the dynamics of the vorticity centroid of each vortex (terms containing y_{ci}) and the second is related to

the unsteady motion of the core fluid relative to this centroid (terms containing y_i''). It has been shown by Tang and Ko [18] that the latter is strongly associated with the core deformation. Eqs. (8) and (9) generalize the results of Tang and Ko [18] to different two-dimensional vortex systems.

In Tang and Ko [18], one can define the impulse centre of an individual vortex, $\boldsymbol{y}_{ic}{}'$, as

$$y'_{ic1} = \oint \omega y'_2 y'_1 \, \mathrm{d}A / \oint \omega y'_2 \, \mathrm{d}A \text{ and } y'_{ic2} = \oint \omega y'_2 y'_1 \, \mathrm{d}A / \oint \omega y'_1 \, \mathrm{d}A,$$

so that

$$\oint \omega y''_1 y''_2 \, \mathrm{d}A = y'_{c2} \oint \omega \, \mathrm{d}A (y'_{ic1} - y'_{c1}) \quad \text{or} \quad y'_{c1} \oint \omega \, \mathrm{d}A (y'_{ic2} - y'_{c2}). \tag{10}$$

Eq. (10) suggests that the sound generated by vortex core deformation can be estimated using the impulse centre and the vorticity centroid of the vortex core.

2.2.2. Vortex rings

The vortex rings are axisymmetrical structures, thus forming a compact vortex system. The system can be described using the cylindrical co-ordinates (z, r, θ) as shown in Fig. 2. $f(\boldsymbol{y})$ here equals $\hat{\theta}/r$, where $\hat{\theta}$ is an unit vector in the azimuthal direction. One obtains

$$p(\boldsymbol{x}, \tau) = \frac{\rho_0}{4c^2|\boldsymbol{x}|}(\cos^2\theta - 1/3)\frac{\partial^3}{\partial\tau^3} \oint \omega r^2 z \, \mathrm{d}A, \tag{11}$$

where the integral is taken over by a cross-section of the vortex system [15]. The time derivative is evaluated at the retarded time $t = \tau - |\boldsymbol{x}|/c$. A quadrupole sound field is created. The source term is $S_r = \oint \omega r^2 z \, \mathrm{d}A$. Suppose the vortex ring system vorticity centroid z_{sc}, which is defined in the same way as $\boldsymbol{y}_{sc}$ (Eq. (6)), is moving in the longitudinal direction z with an unsteady speed, then $S_r = \oint \omega r^2 z \, \mathrm{d}A = \oint \omega r^2 (z' + z_{sc}) \, \mathrm{d}A$, where z' represents a longitudinal distance relative to z_{sc}. Owing to the conversation of vortex impulse, the quadrupole source strength is

$$\frac{\partial^3 S_r}{\partial t^3} = \frac{\partial^3}{\partial t^3} \oint \omega r^2 z' \, \mathrm{d}A + \oint \omega r^2 \, \mathrm{d}A \frac{\partial^3 z_{sc}}{\partial t^3}. \tag{12}$$

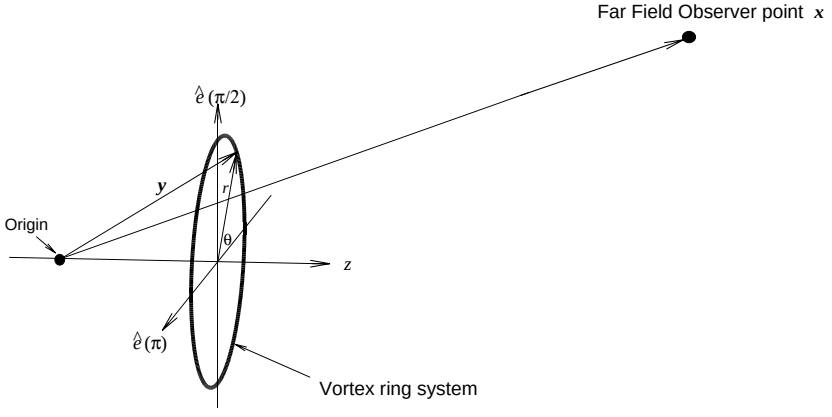

Fig. 2. Schematic diagram for vortex ring system.

Concerning the farfield contribution of an individual vortex ring, one can define the vorticity centroid of one of the vortex ring (z'_c, r_c) as

$$r_c = \oint \omega r \, \mathrm{d}A / \oint \omega \, \mathrm{d}A \quad \text{and} \quad z'_c = \oint \omega z' \, \mathrm{d}A / \oint \omega \, \mathrm{d}A, \tag{13}$$

where the integrals are taken over the core of the vortex ring concerned. It follows that the farfield pressure contribution from one vortex ring is

$$\frac{\partial^3 S_r}{\partial t^3} = \frac{\partial^3}{\partial t^3}\left(\oint \omega r''^2 z'' \, \mathrm{d}A + 2r_c \oint \omega r'' \, \mathrm{d}A + z'_c \oint \omega r''^2 \, \mathrm{d}A \right) + \oint \omega \, \mathrm{d}A \frac{\partial^3}{\partial t^3} r_c^2 z'_c + \oint \omega r^2 \, \mathrm{d}A \frac{\partial^3 z_{sc}}{\partial t^3}, \tag{14}$$

where $''$ denotes quantity relative to the vorticity centroid. The last two terms on the right-hand side of Eq. (14) represents sound generation by vortex centroid dynamics, while the other three are the contributions from fluid motions relative to the centroid. The latter relates to core deformation. This is consistent with the deduction from Eq. (9) for the case of two-dimensional vortex system.

One can also define the impulse centre of an individual vortex ring, (z'_{ic}, r_{ic}), according to Lamb [24]:

$$r_{ic} = \sqrt{\oint \omega r^2 \, \mathrm{d}A / \oint \omega \, \mathrm{d}A} \quad \text{and} \quad z'_{ic} = \oint \omega r^2 z' \, \mathrm{d}A / \oint \omega r^2 \, \mathrm{d}A, \tag{15}$$

which can be computed by contour integrals. It follows that

$$\frac{\partial^3}{\partial t^3}\left(\oint \omega r''^2 z'' \, \mathrm{d}A + 2r_c \oint \omega r'' \, \mathrm{d}A + z'_c \oint \omega r''^2 \, \mathrm{d}A \right) = \frac{\partial^3}{\partial t^3} \oint \omega \, \mathrm{d}A (r_{ic}^2 z'_{ic} - r_c^2 z'_c). \tag{16}$$

Eq. (16) is an analogue of Eq. (10) for an vortex ring system. Eqs. (14) and (16) further generalize the deductions of Tang and Ko [18] to the axisymmetrical vortex system. The theory shows the importance of the offset between impulse centre and vorticity centroid, which is due to the distortion of vortex ring core from its steadily propagation shape [25], in the sound generation process.

2.2.3. *Similarities in sound generation mechanisms*

Though the two-dimensional vortices and the vortex rings are different in nature, one can observe from the derivations in the previous two sections that the sources of sound during their interactions are similar. For the two-dimensional vortices and vortex pairs, Eq. (9) suggests that the unsteady dynamics of the vorticity centroids and the motions of the core fluids relative to the vorticity centroids are the two basic mechanisms for sound generation. The latter is shown to relate to the spatial location differences between impulse centres and the vorticity centroids, which vanish or are constants in the case of steady vortex motions (Eq. (10)). Therefore, the second mechanism can be regarded as the unsteady core deformation.

For vortex rings, Eq. (14) shows explicitly the importance of vorticity centroid dynamics and the unsteady motions of core fluids relative to the vorticity centroids in the production of sound. The source terms related to the latter mechanism can be grouped into one single term concerning

impulse centres and vorticity centroids (Eq. (16)). The difference $(r_{ic}^2 z'_{ic} - r_c^2 z'_c)$ is time-invariant for a steady propagating vortex ring. Thus, this difference represents the effects of core deformation (deviation for steady propagating state) in the production sound. Therefore, it can be concluded that, whether the system is two-dimensional or ring-type (axisymmetrical), the sound produced is due to two mechanisms. The first one is the unsteady vorticity centroid dynamics and the other the unsteady deformation of vortex cores. It will be shown later that the sound produced by these mechanisms possess similar features, regardless of the interaction systems.

Though the expressions of the sound source terms for the two-dimensional and axisymmetric vortex systems look different, their physical meanings are almost the same. The source terms due to vorticity centroid dynamics are $y_{c1} y_{c2} \oint \omega \, \mathrm{d}A$ and $r_c^2 z'_c \oint \omega \, \mathrm{d}A$ for the two-dimensional and axisymmetric systems, respectively. The latter involves the impulse of the vortex ring in the axial direction ($r_c^2 \oint \omega \, \mathrm{d}A$), while the former the impulse of the two-dimensional vortex and vortex pair in the longitudinal direction ($y_{c2} \oint \omega \, \mathrm{d}A$). Thus, the time derivatives of these terms are related to the rates of change of the internal forces magnitudes, their work done and the axial/longitudinal jerking motions of the vortices. Concerning the source terms due to the core deformation, the term $(y'_{ic1} - y'_{c1}) y'_{c2} \oint \omega \, \mathrm{d}A$ in the two-dimensional system (Eq. (10)) represents the unbalance of the longitudinal vortex impulse at the vorticity centroid. The interpretation of the corresponding term in the axisymmetric system, $(r_{ic}^2 z'_{ic} - r_c^2 z'_c) \oint \omega \, \mathrm{d}A$, is not that straightforward. However, it does represent the extra vortex ring impulse due to an offset between the impulse centre and the vorticity centroid. Similar to the term $(y'_{ic1} - y'_{c1}) y'_{c2} \oint \omega \, \mathrm{d}A$, it depends on the deformation of vortex core from its equilibrium shape. Thus, sound generation mechanisms described by these two terms are similar, though the forms look different.

The following sections illustrate the generality of the above-derived sound generation mechanisms in the commonly observed major vortex interactions in plane and axisymmetric shear flows. They are leapfrogging, coalescence and collision. The effects of mean flows are ignored for simplicity.

3. Numerical results and discussions

This section is to illustrate the similarities of the sound generation mechanisms in the interactions of two-dimensional vortices, vortex pairs and vortex rings. For the two-dimensional vortices, the initial cores are assumed to be circular, while those for the vortex pairs and vortex rings follow the steadily translating solutions given by Pierrehumbert [26] and Norburg [25], respectively. In order to give a detailed analysis on the basic mechanisms of sound generation in different vortex interaction systems, the strengths of the interacting vortices are set to be different. In the following sub-sections for the two-dimensional systems, ω_s and ω_w denote the vorticity inside the stronger and weaker vortex, respectively. For vortex rings, these parameters denote the corresponding vorticity at the initial locations of the vorticity centroids.

3.1. Leapfrogging

Leapfrogging interaction between vortices is commonly found in the initial regions of low-Mach-number mixing layers and is believed to be responsible for the growth of the layers [27].

In a plane mixing layer, the initial coherent structures can be modelled as two-dimensional vortices. When the vortices are well separated, their vorticity centroids undergo leapfrogging motions having nominally circular orbits [13]. For this type of vortex system motions, the system vorticity centroid is stationary and thus, all the terms on the right-hand side of Eq. (8) associated with the time differentiation of $\boldsymbol{y}_{sc}$ vanish. In the foregoing discussions, σ denotes the radius of the initial vortex core and is taken to be the same for each interacting vortex.

Fig. 3 shows typical examples of the time variations of the sound source strength $\partial^3 S_1/\partial t^3$ and the contributions of the core deformation and the macroscopic vorticity centroid dynamics associated with the two-dimensional vortex leapfrogging motions ($\omega_w/\omega_s = 0.866$). For both vortices, the unsteady vorticity centroid dynamics produce a relatively low-frequency sound. This

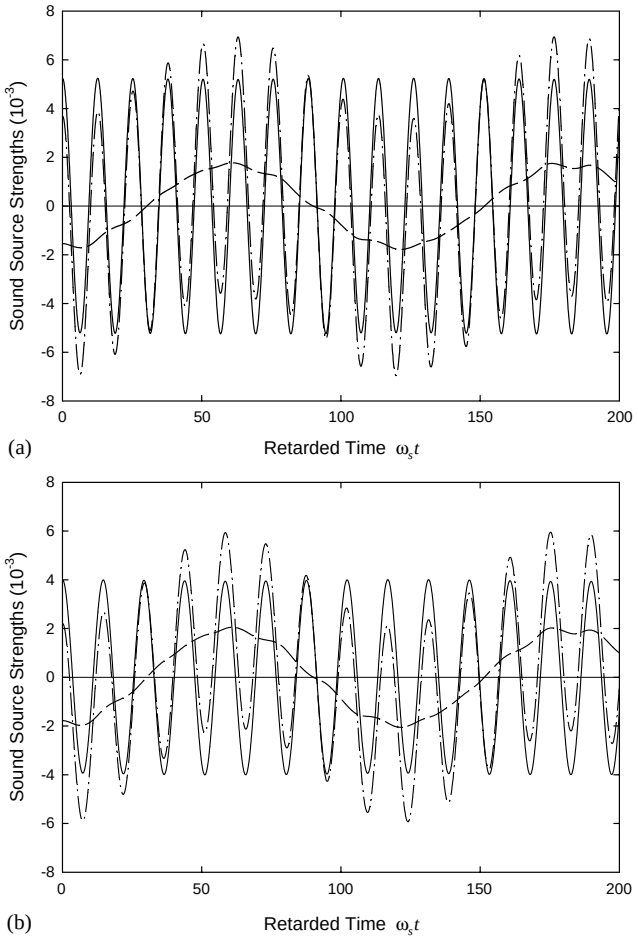

Fig. 3. Time variations of source strengths during two-dimensional vortex leapfrogging. $G/\sigma = 6$, $\omega_w/\omega_s = 0.866$. (a) Stronger vortex and (b) weaker vortex. (—) Contribution from core deformation; (— —) contribution from vortex centroid dynamics; (—·—) overall contribution from individual vortex.

frequency is close to the rotational speed of the centroids and is the same for both vortices. It is observed that the corresponding motion of the weaker vortex produces higher low-frequency sound magnitude. The source strength related to the core deformation, $\partial^3/\partial t^3 \oint \omega y_{12}'' \, dA$ in Eq. (9a), gives rise to high-frequency sinusoidal oscillations. The stronger the vortex, the greater the magnitude and frequency of these oscillations. The peaks and troughs of these oscillations are found at the instant when the rates of vortex core deformation are high [13]. Similar observations can be made for $\partial^3 S_2/\partial t^3$ and thus the corresponding results are not presented. If one represents the vortex system using polar co-ordinates with the origin set at the current vortex system centroid, it is straightforward to verify that $\partial^3 S_1/\partial t^3$ and $\partial^3 S_2/\partial t^3$ for each vortex are only 90° out-of-phase with each other. This suggests that they come from the same mechanisms. Therefore, the following discussions in this section will be focussed only on $\partial^3 S_1/\partial t^3$.

It can be also observed from Fig. 3 that the frequencies of the high-frequency oscillations produced by the stronger and weaker vortices are in the ratio of 1:0.866. This is consistent with the vorticity ratio ω_w/ω_s. Such observation indicates that the sound generated by unsteady core deformation of a particular vortex is related to its own strength, that is, its own circulation. The higher the circulation, the higher is this frequency.

The difference in these high-frequency oscillation frequencies results in the formation of beats in the far field (Fig. 4), though the contributions of the vortical elements along the y_3 direction, which arrive at the far field at different time intervals, may to some extent smoothen the farfield pressure fluctuations. Fig. 4 also indicates that the two sound generation mechanisms of core deformation and vorticity centroid dynamics are basically independent of each other, as one can

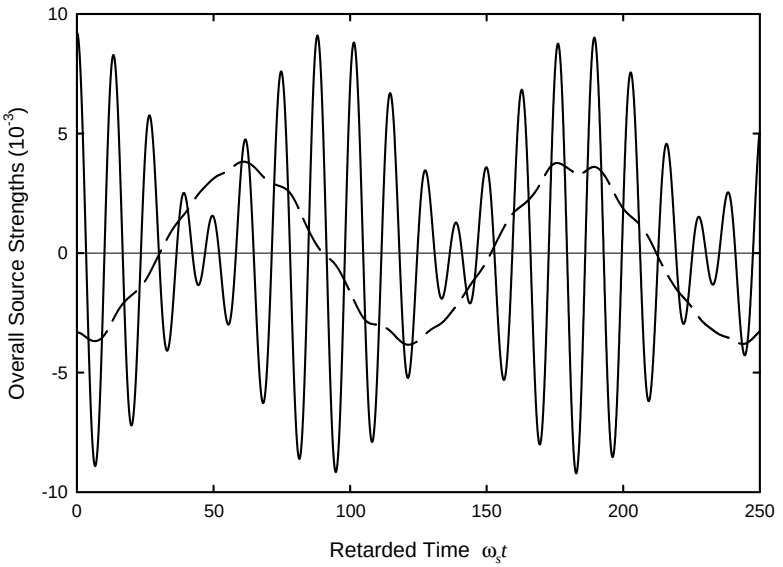

Fig. 4. Time variations of overall source strengths of two-dimensional vortex leapfrogging. $G/\sigma = 6$, $\omega_w/\omega_s = 0.866$. (—) Contribution from core deformation; (— —) contribution from vortex centroid dynamics.

find large low-frequency sound generation at the instants of high and weak high-frequency sound production.

The vortex pairs dominate the initial regions of low-Mach-number two-dimensional jets or rectangular jets with large aspect ratios. In theory, a vortex pair is characterized by a variable α, which represents the ratio of the equivalent vortex core radius to the separation of the two vortex centroids in the vortex pair d [26]. Without loss of generality, the two interacting vortex pairs are taken to have the same d and α initially. Unlike the case for two-dimensional vortex leapfrogging, the overall source strength $\partial^3 S_2/\partial t^2$ vanishes as the contributions from the vorticity patches cancel each other completely.

Leapfrogging of vortex pairs is observed with $G/d = 2.85$, $\alpha = 0.6$ and $\omega_w/\omega_s = 0.866$, where G is the initial separation between the vortex pairs (not shown here). The system vorticity centroid is translating with a steady speed along the y_1-axis. Thus, all the terms on the right-hand side of Eq. (8) involving the time differentiation of $\boldsymbol{y}_{sc}$ again vanish or have negligible effects. Again, one can find that the rectilinear point vortex model [28], which does not take into account any form of vortex core deformation, can predict the low-frequency pulses which are generated close to the slip-through instants by the unsteady vorticity centroid dynamics (Fig. 5). The high-frequency fluctuations are due to the vortex core deformation. As the sound generation mechanisms have been studied in detail by Tang and Ko [18], except that no comparison with the point vortex model prediction was given by the two researchers; no further discussion will be given in the present paper. However, the frequency of the high-frequency fluctuation produced by the stronger vortex pair is higher than that associated with the weaker pair. The frequency ratio is again 0.866, the same as the ratio ω_w/ω_s (Fig. 6). It should be noted that the magnitudes of the spectral

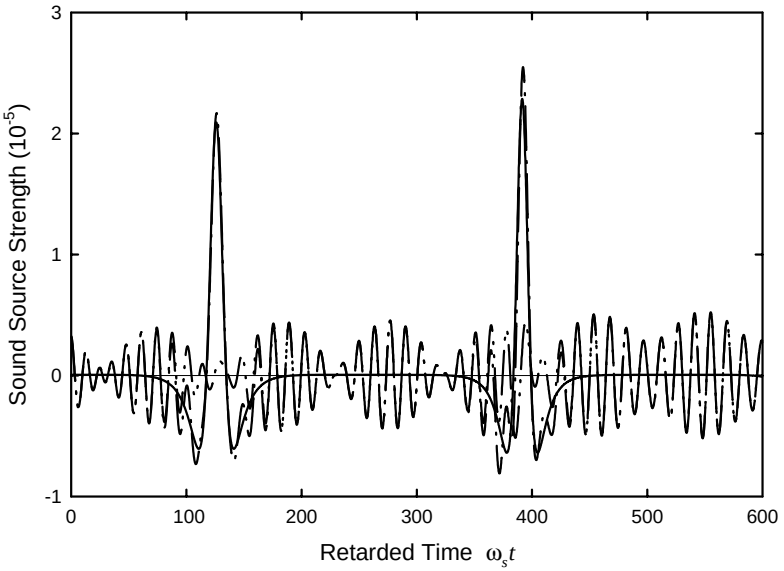

Fig. 5. Time variations of overall source strengths of vortex pair leapfrogging. $G/d = 2.85$, $\omega_w/\omega_s = 0.866$, $\alpha = 0.6$. (—) Rectilinear vortex model prediction [28]; (—·—) overall source strength of the system; (—· ·—) effect of core deformation.

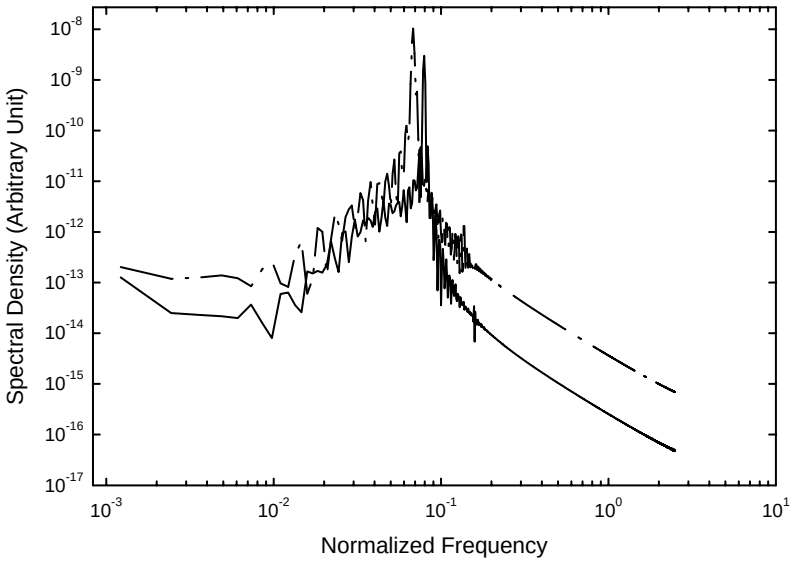

Fig. 6. Frequency characteristics of source strengths due to core deformation of vortex pair leapfrogging. $G/d = 2.85$, $\omega_w/\omega_s = 0.866$, $\alpha = 0.6$. (—) Stronger vortex; (—·—) weaker vortex.

densities illustrated in Fig. 6 only reveal the averaged magnitudes of the frequency peaks as they vary with the time of flight of the vortex pairs. This is not the case in two-dimensional vortex leapfrogging (Fig. 3).

In low-Mach-number axisymmetric jets, the coherent structures are the vortex rings. The unsteadily interacting vortex rings form a compact sound generation system. Without loss of generality, the initial radii, R, of the interacting vortex rings in the present computation are taken to be the same. The initially leading vortex ring is set to be the weaker one. β denotes the ratio of the equivalent core radius to the ring radius in the Norburg's system [25].

With the appropriate G/R, the vortex rings having the same sense of core fluid rotation undergo the well-known leapfrogging motion, also known as the mutual slip-through motion [29]. The interacting vortex ring system is, again, translating with a constant speed, though the velocities of individual vortex rings are different. The second term on the right-hand side of Eq. (12), therefore, vanishes. Fig. 7 illustrates a typical example of the time variations of the source strength fluctuations of $G/R = 0.5$ and $\omega_w/\omega_s = 0.866$, as calculated using Eqs. (12) and (16), during a vortex ring leapfrogging. Similar to the case of vortex pair leapfrogging, the activities of the core fluids relative to the vorticity centroids, which are ascribed to be the result of unsteady core deformation, produce high-energy high-frequency source strength fluctuations. The stronger the vortex ring, the larger the magnitude of these fluctuations. The dynamics of the vorticity centroids generate lower frequency source strength fluctuations, which are of importance close to the instants of vortex ring slip-through. It has been shown by Tang and Ko [15] that this strong sound radiation at the slip-through instants is due to the radial acceleration of the vorticity centroid and will not be discussed further here. Also, smaller magnitude high-

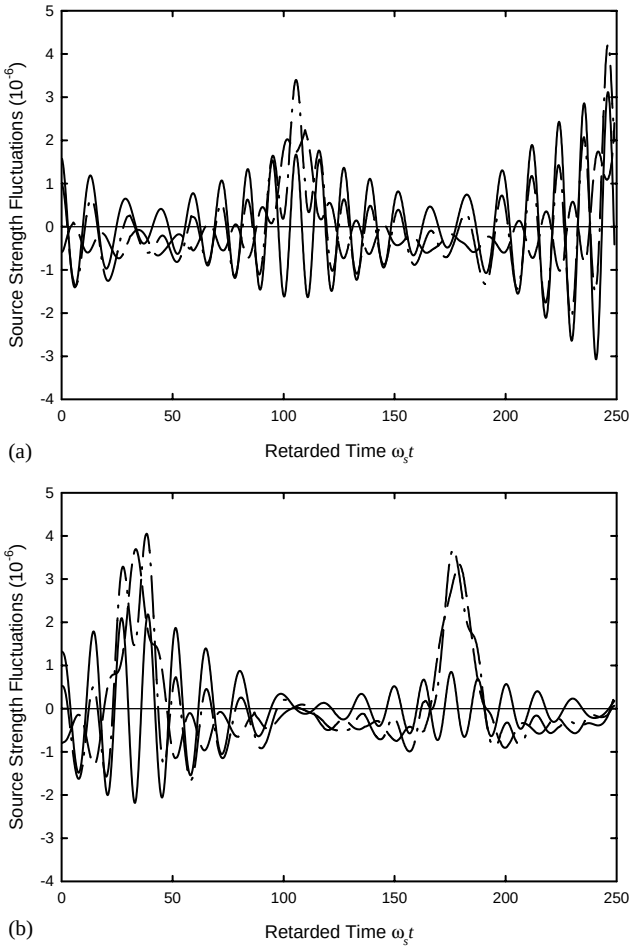

Fig. 7. Time variations of source strengths of vortex ring leapfrogging. $G/R = 0.5$, $\omega_w/\omega_s = 0.866$, $\beta = 0.1$. (a) Stronger vortex ring and (b) weaker vortex ring. (—) Contribution from core deformation; (— —) contribution from vortex centroid dynamics; (— · —) overall contribution from individual vortex.

frequency fluctuations are found on the source strength fluctuations produced by the macroscopic dynamics of the vorticity centroids due to the core deformation as in the cases of the two-dimensional vortices and vortex pairs. A comparison between results obtained from the present contour dynamics computation and the Dyson model is shown in Fig. 8 [30]. This model assumes circular cores with constant vorticity throughout the interaction and is only able to predict the slowly varying pulses produced at the slip-through instants. In addition, the high-frequency source strength fluctuations produced by the stronger vortex ring have a higher frequency than that associated with the weaker one. The frequency ratio is again 1:0.866 (Fig. 9), showing that these high-energy sound sources are mainly due to the self-induction within the cores.

It is interesting to note from Fig. 7 that the magnitudes of the source strengths of the unsteady core fluid motions relative to individual vorticity centroids vary substantially with time. The

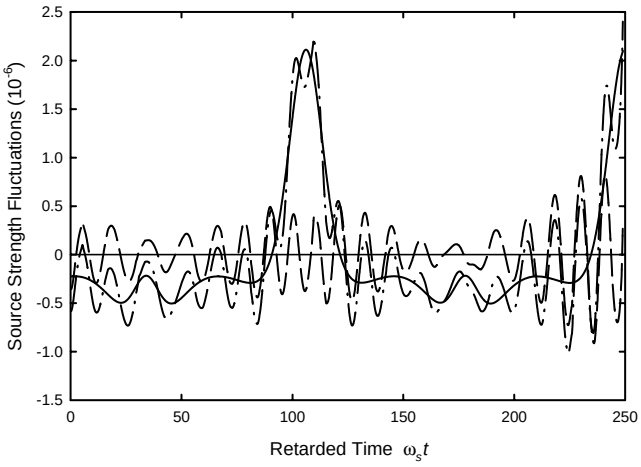

Fig. 8. Effects of core deformation on sound generation by vorticity centroid dynamics of stronger vortex ring during vortex ring leapfrogging. $G/R = 0.5$, $\omega_w/\omega_s = 0.866$, $\beta = 0.1$. (—) Dyson model prediction [30]; (— · —) source strength due to vorticity centroid dynamics; (— —) effect of core deformation.

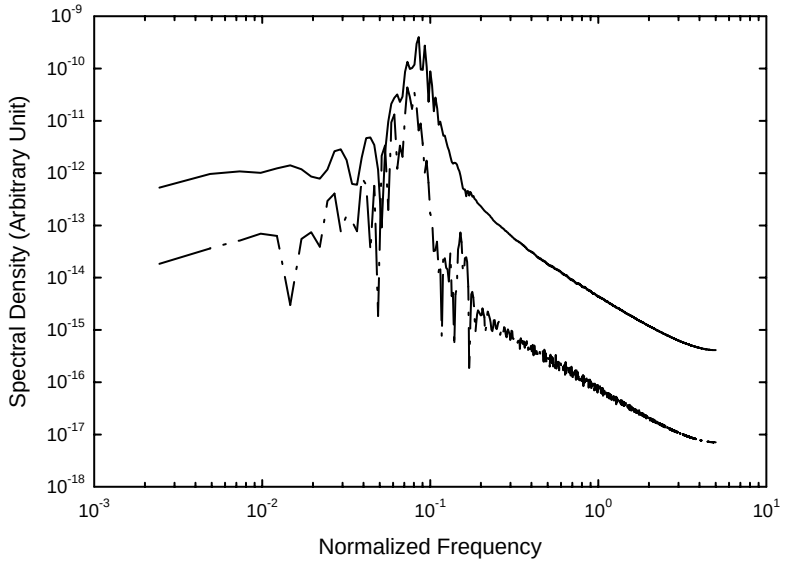

Fig. 9. Frequency characteristics of source strengths due to core deformation of vortex ring leapfrogging. $G/R = 0.5$, $\omega_w/\omega_s = 0.866$, $\beta = 0.1$. Legends: same as those in Fig. 6.

minima for each vortex ring are observed at instants when the ring radius is the smallest, while the maxima occur at instants of greatest ring radius. This is not observed in the vortex pair leapfrogging case, where the magnitudes of the high-frequency source strength fluctuations are nearly time-invariants. One should note that the vortex ring core size changes during the interaction, though the circulation of each vortex ring remains unchanged. According to the vortex sound theory (Eq. (14)) and the previous results of the authors [15], the production of

sound is highly related to the impulse of each vortex ring, which is proportional to Γr_{ic}^2. As a vortex ring squeezes through another vortex ring, its impulse decreases with the square of its radius, resulting in weaker sound generation. Also, the vorticity at a point inside a vortex ring of the Norbury's family is proportional to the radial position of the point concerned [25]. One can, therefore, expect from Eq. (16) that a decrease of the mean vortex ring radius leads to weaker high-frequency source strength production. This is not the case for the vortex pairs or the two-dimensional vortices, where the size of and the vorticity inside each vortex are time-invariants.

It can be concluded that there are two independent sound sources in the leapfrogging vortex interactions, regardless of the type of vortex system. The macroscopic vorticity centroid motions produce a low-frequency sound, while the unsteady core deformation results in higher frequency farfield pressure fluctuations. The latter is directly related to self-induction.

3.2. Collisions

Collision interaction occurs when two vortices of opposite circulation come close to each other. Some examples of this interaction can be found in the wakes of cylinder flows [31] and in coaxial jets [32]. Since collision does not occur in a single plane mixing layer, only vortex pairs and vortex rings will be considered in this sub-section. Vortex coalescence during collision involves substantial vortex stretching, which cannot be modelled by the contour dynamics model. Thus, it is excluded in the present study.

During a head-on collision of two vortex pairs having the same strength but with opposite sense of vortex core fluid rotation, the two vortex pairs originally moving towards each other in the y_1 direction eventually move away from each other in the y_2 direction (not shown here). All vortex core boundaries remain well separated and the system vorticity centroid is stationary. Again, the time fluctuation of the source strength $\partial^3/\partial t^3 \oint \omega y_{12}'' \, \mathrm{d}A$ resulted from core deformation is sinusoidal. Fig. 10 shows a typical example of the phenomenon with $G/d = 4$, $\alpha = 0.5$ and $|\omega_w/\omega_s| = 1$. Though the vorticity centroid dynamics produce sound of much lower frequency, the sound does contain some small magnitude high-frequency fluctuations, which are 180° out-of-phase with those produced by core deformation. Fig. 11 compares the sound produced by the corresponding vorticity centroid dynamics with that predicted by the rectilinear point vortex model [28]. It is clearly illustrated that the small magnitude source strength fluctuations produced by the vorticity centroid dynamics are due to the effects of core deformation. The vortex core deformation gives rise to significantly high-frequency vorticity centroid jerking motions, creating the above-mentioned small magnitude source strength fluctuations (not shown here).

When the colliding vortex pairs possess different strengths, the colliding system vorticity centroid moves with an unsteady velocity parallel to the axes of the vortex pairs. The sound source strength is, according to Eq. (8a),

$$\frac{\partial^3 S_1}{\partial t^3} = \frac{\partial^3}{\partial t^3} \oint \omega y_1' y_2' \, \mathrm{d}A + \oint \omega y_2' \, \mathrm{d}A \frac{\partial^3 y_{sc1}}{\partial t^3}.$$

The unsteady jerking motion of the system vorticity centroid produces additional sound.

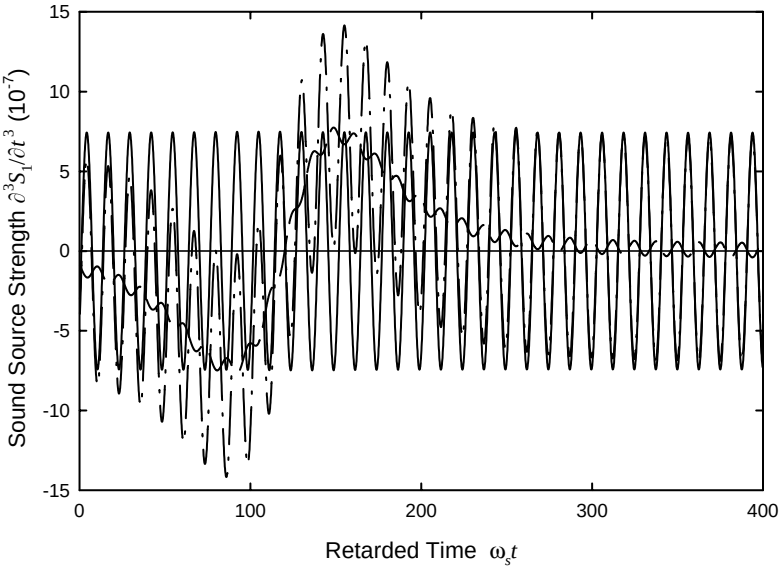

Fig. 10. Sound source strength fluctuations of vortex pair head-on collision. $G/d = 4$, $\alpha = 0.5$. Legends: same as those in Fig. 3.

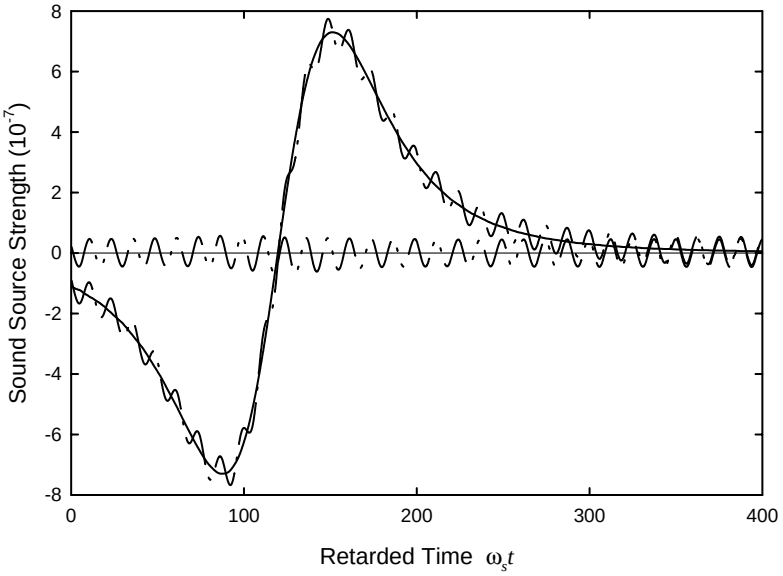

Fig. 11. Effects of core deformation on sound generation by vorticity centroid dynamics during vortex pair head-on collision. $G/d = 4$, $\alpha = 0.5$. (—) Rectilinear vortex model prediction [28]; (—·—) source strength due to vorticity centroid dynamics; (— —) effect of core deformation.

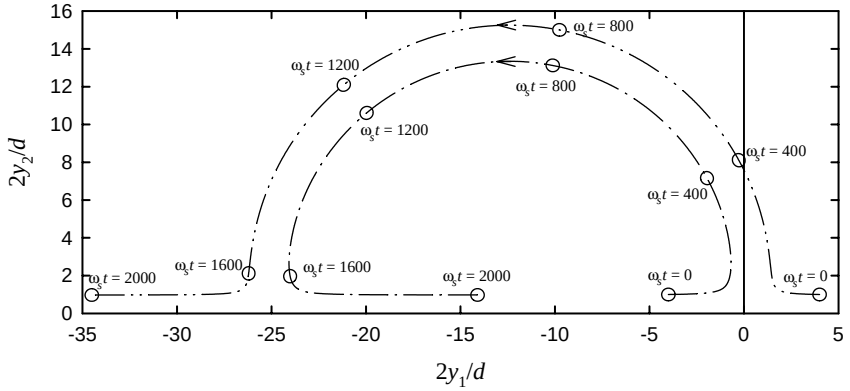

Fig. 12. Vortex dynamics during collision between unequal vortex pairs. $G/d = 4$, $|\omega_w/\omega_s| = 0.866$, $\alpha = 0.5$. (—) Vortex cores; (— · —) trajectory of stronger vortex vorticity centroid; (— · · —) trajectory of weaker vortex vorticity centroid. Arrow denotes direction of motion.

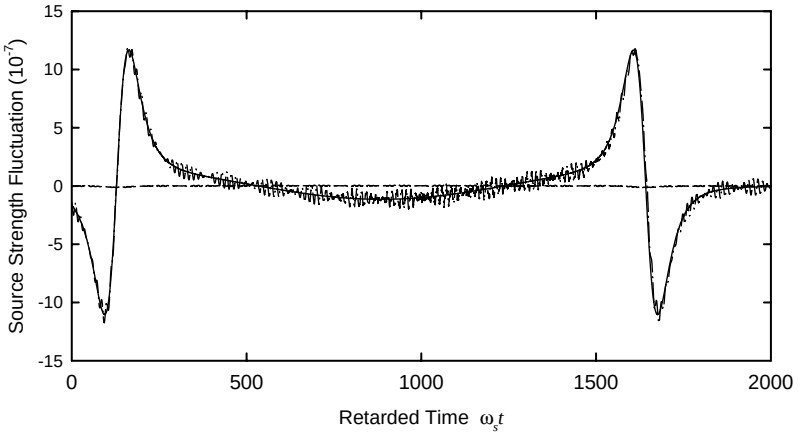

Fig. 13. Overall sound source strength fluctuations of unequal vortex pair collision. $G/d = 4$, $|\omega_w/\omega_s| = 0.866$, $\alpha = 0.5$. (—) Rectilinear model prediction [28]; (— · —) overall source strength of the system; (— —) effect of unsteady system vorticity centroid motion.

A typical example of the unequal vortex pair collision is illustrated in Fig. 12 ($G/d = 4$, $\alpha = 0.5$ and $|\omega_w/\omega_s| = 0.866$). The cores of the vortex pairs are moving under the close influence of each other after the first collision at $y_1/d \approx 1$. The vortex cores on the positive y_2-plane move like a vortex dipole. The second collision takes place at $y_1/d \approx -25$, but in the transverse direction. The vortex pairs eventually move in the opposite directions. This kind of double collision is not observed in the case of vortex ring collision studied by Tang and Ko [16]. This is due to the weak self-induced velocity field within each vortex pair.

Again, the time variations of source strengths contain a low-frequency component and a much higher frequency component, while the effect of y_{sc1} is very small (Fig. 13). The low-frequency

component is important at the instant close to each collision, during which there is an approximately 90° change in the core motion direction. Beats are found on the overall source strength time fluctuations (Fig. 13). Again, the rectilinear vortex model [28] only predicts the low-frequency source strength time variation but not the small magnitude high-frequency fluctuations, which are due to the effect of core deformation. Similar to the cases of the two-dimensional vortex interaction and of the vortex pair leapfrogging discussed earlier, for collision the frequency of the high-frequency fluctuations produced by the weaker vortex pair is about 0.866 times that of the stronger vortex pair (Fig. 14).

Two vortex rings initially moving towards each other undergo a collision interaction, as investigated by Tang and Ko [16] numerically and by Kambe and Minota [33] both theoretically and experimentally. In general, their results on the time variations of farfield pressure fluctuations are consistent with each other. In addition, Tang and Ko [16] have pointed out the importance of vortex ring jerks and accelerations in the production of sound by the vortex ring collision process. Without loss of generality, the initial radii of the colliding vortex rings in the present investigation are taken to be the same.

During a head-on collision of two vortex rings, the vortex ring cores are close to each other at increased flight time, due to the strong self-induced forward going velocities. The second term on the right-hand side of Eq. (12) vanishes as $z_{sc}/R \equiv 0$. An example of the sound source variations with $G/R = 4$, $\beta = 0.2$ and $|\omega_w/\omega_s| = 1$ is given in Fig. 15. The core deformation again results in the generation of higher frequency source strength fluctuations. The magnitude of this sinusoidal fluctuations increases as the cores get closer to each other. The degree of core deformation also becomes more serious. The dynamics of the vorticity centroids are affected by the core deformation so that small magnitude high-frequency source

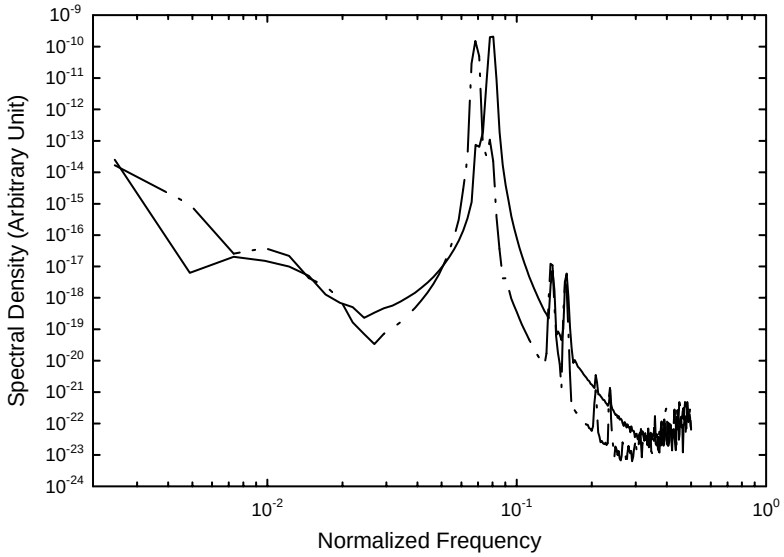

Fig. 14. Frequency characteristics of source strengths due to core deformation of unequal vortex pair collision. $G/d = 4$, $|\omega_w/\omega_s| = 0.866$, $\alpha = 0.5$. Legends: same as those in Fig. 6.

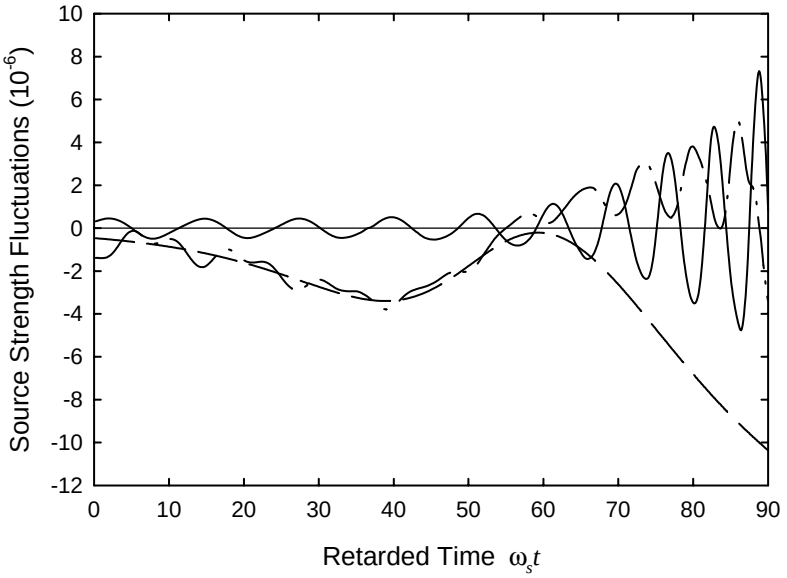

Fig. 15. Sound source strength fluctuations of vortex ring head-on collision. $G/R = 4$, $\beta = 0.2$. (—) Direct contribution from core deformation; (— · —) overall source strength fluctuations; (— —) Dyson model prediction [30].

strength fluctuations are observed on the relatively low-frequency source strength time variation. The Dyson circular core model [30] predicts the low frequency source strength fluctuations only for $\omega_s t < 51$, when the vortex ring cores are slightly deformed from their steadily translating shapes. Once the vortex cores are severely deformed, the Dyson model [30] can no longer predict the motions of the vortex rings and the sound production. This is consistent with the observation of Shariff et al. [34].

For unequal vortex ring collision, the two colliding vortex rings basically maintain its original longitudinal direction of motion, even when the vortex cores are close to each other due to strong self-induction fields [16]. Fig. 16 illustrates the sound source strengths obtained from a vortex ring collision with $G/R = 4$, $\beta = 0.2$ and $|\omega_w/\omega_s| = 0.333$. The high-frequency source strength fluctuations are the results of unsteady core deformations, though the amplitudes of those produced by the weaker vortex ring are small. However, it should be noted that while the significantly high-frequency source strength fluctuations are produced by the stronger vortex ring, the large negative pulse generated close to the slip-through instant ($\omega_s t = 105.2$) is due to the dynamics of the weaker vortex ring vorticity centroid. The high radial acceleration of the vortex ring has been found to be the major sound production mechanism during this short period of time [16]. The predictions of the Dyson model [30] are basically the same as those illustrated in Fig. 16, without the high-frequency components and thus are not presented.

In this section, it is again found that the sound produced by core deformation, be it of two-dimensional vortices and vortex rings, during vortex collision is of high frequency, while that due to the unsteady vorticity centroid dynamics varies slowly with time. The two sound sources are

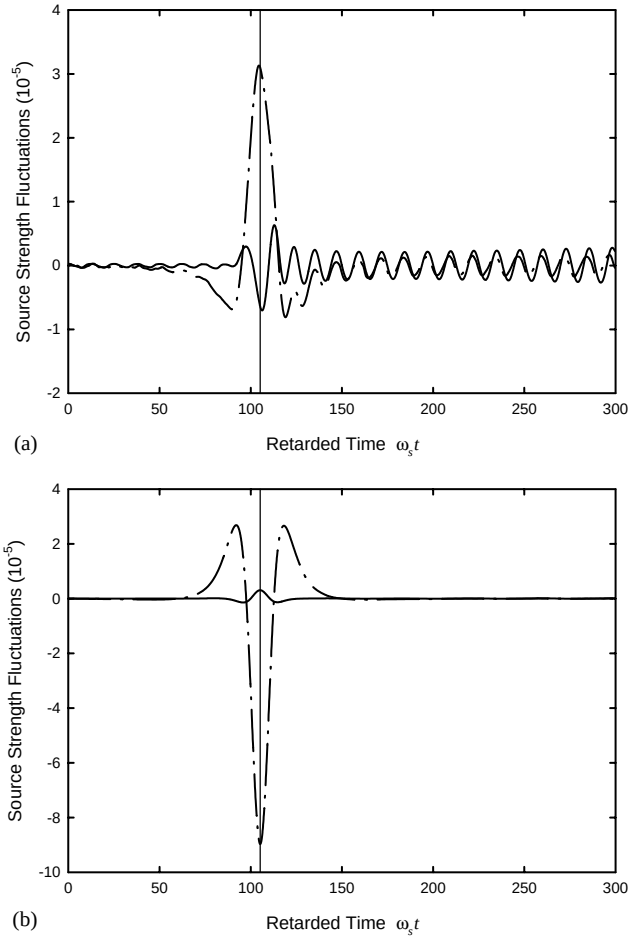

Fig. 16. Time variations of source strengths of unequal vortex ring collision. $G/R = 4$, $|\omega_w/\omega_s| = 1/3$, $\beta = 0.2$. (a) Stronger vortex ring and (b) weaker vortex ring. (—) Direct contribution from core deformation; (—·—) overall contribution from individual vortex ring.

independent of each other. Similar to the case for vortex leapfrogging, the high-frequency sound is produced by self-induction.

3.3. Coalescence

Vortex coalescence is the last stage of vortex pairing during which two vortical structures merge into a single structure [27,29]. This interaction is usually found in plane and axisymmetric mixing layers. In theory, the cores of the inviscid vortices cannot come into mutual contact. Thus, coalescence in this presentation is defined as the mutual folding together of the cores of the interacting vortices [35]. Serious core deformation occurs.

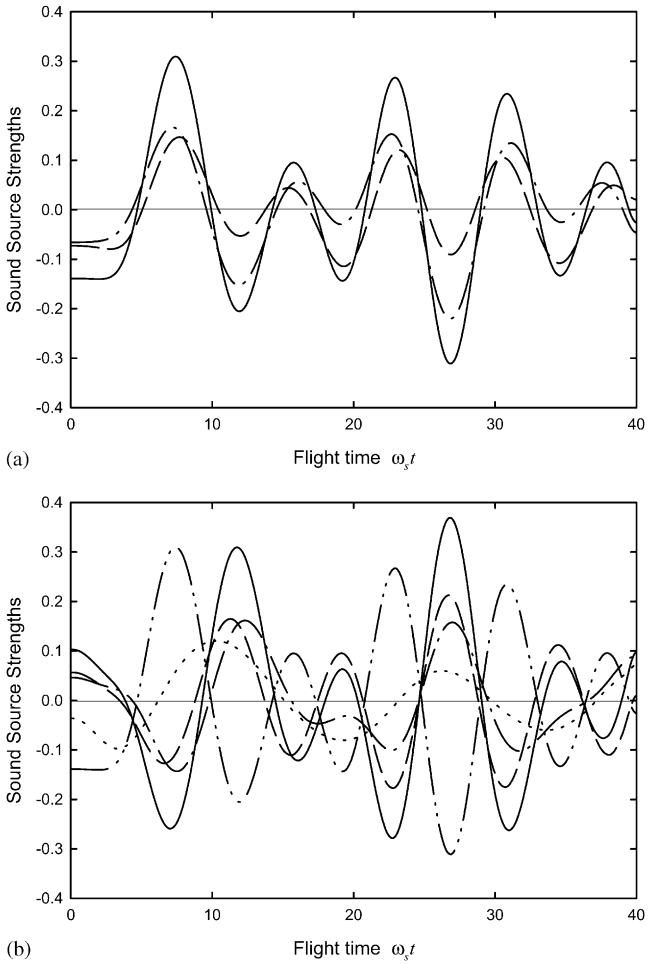

Fig. 17. Sound source strength fluctuations of two-dimensional vortex coalescence. $G/\sigma = 2.5$, $\omega_w/\omega_s = 0.866$. (a) Contributions from vorticity centroid dynamics. (—) Total contribution from vorticity centroid dynamics; (— · —) stronger vortex; (— —) weaker vortex. (b) Contributions from unsteady core deformation. (……) Overall source strength; (— · · —): total contribution from vorticity centroid dynamics; (—) total contribution from unsteady core deformation; (— · —) contribution from core deformation of stronger vortex; (— —) contribution from core deformation of weaker vortex.

The discussions will be focused on the terms $\partial^3 S_1/\partial t^3$ and $\partial^3 S_r/\partial t^3$ for the two-dimensional systems and the axisymmetric system, respectively, since $\partial^3 S_2/\partial t^3$ is 90° out-of-phase with the $\partial^3 S_1/\partial t^3$ in the two-dimensional vortex interaction and vanishes in vortex pair interaction. Fig. 17a shows the typical time fluctuations of the source strengths due to the unsteady vorticity centroid dynamics during the two-dimensional vortex coalescence. The contribution from each vortex is approximately in-phase. Similar phenomenon is observed for the source strengths due to the core deformation (Fig. 17b). However, it can also be noticed that the total contributions from each of the two above-mentioned source mechanisms counteract each other, resulting in the

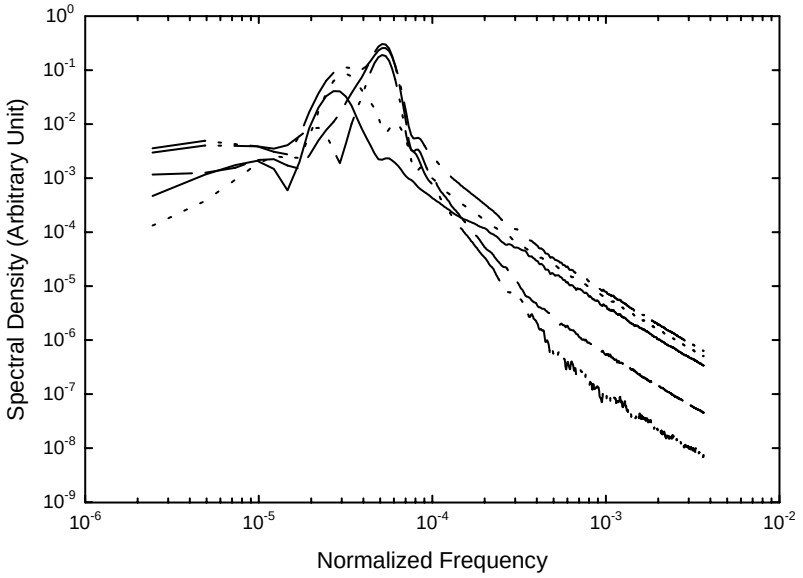

Fig. 18. Frequency characteristics of source strengths of two-dimensional vortex coalescence. Legends: same as those in Fig. 17b.

radiation of a low-frequency sound. As shown by the spectra of the source strengths (Fig. 18), the low-frequency sound comes from the unsteady core deformation of the weaker vortex.

Similar relationships between different source terms are observed during the coalescence of vortex pairs (Fig. 19). Since the core shapes and the time variations of the source terms resemble those of the two-dimensional vortex case. The results are not discussed here.

The source terms due to the vorticity centroid dynamics from the two interacting vortex rings are approximately out-of-phase with each other (Fig. 20a). The difference in their strengths results in the radiation of higher frequency sound. The peaks in the figure occur at the instants when the two vorticity centroids are co-planner, and are associated with the ring of larger radius (not shown here). This is similar to the results of the vortex ring leapfrogging cases (for instance, Fig. 7), though the core deformation in the coalescence is much more serious. This further confirms the vorticity centroid dynamic is one of the basic mechanisms for sound generation in vortex ring interaction.

Fig. 20b illustrates that the source terms due to the unsteady core deformation in coalescence are of a frequency close to that of the overall source term due to the vorticity centroid dynamic. However, one can find that the vorticity centroid dynamic is the dominant sound generation mechanism during the vortex ring coalescence. Unlike the case of vortex pairs and two-dimensional vortices, both the strong and weak vortex rings are important in the overall production of sound (Fig. 21a), with the contribution of the latter slightly higher than that of the former (Fig. 21b).

In this section, examples of sound generation by the coalescence of vortex pairs, two-dimensional vortices and vortex rings are given. Similar results can be obtained with other combinations of vortex separations, circulation ratios, etc. as far as the type of interaction is unchanged. Results indicate again that the unsteady vorticity centroid dynamics and the core

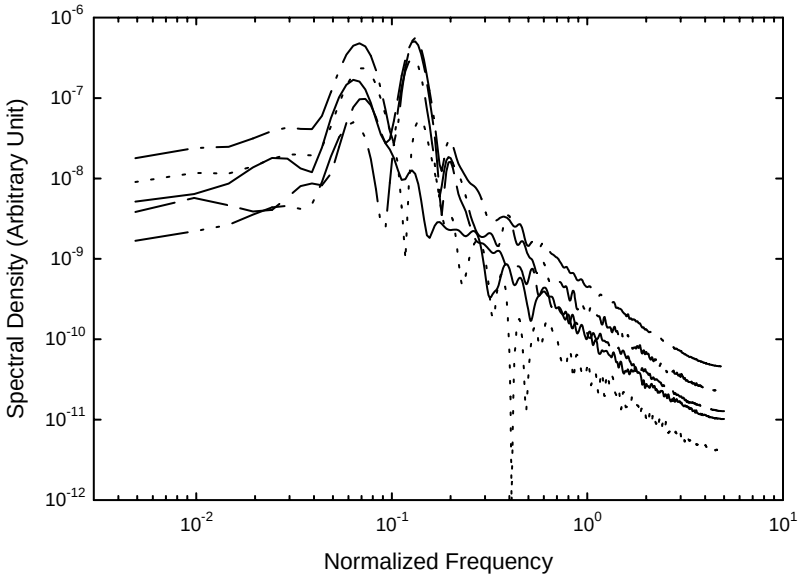

Fig. 19. Frequency characteristics of source strengths of vortex pair coalescence. $G/d = 1$, $\omega_w/\omega_s = 0.866$, $\alpha = 0.5$. Legends: same as those in Fig. 17b.

deformation remain the two basic mechanisms for sound generation. The former is more important in vortex ring interaction, while the latter dominates the sound generation for the two two-dimensional systems.

4. Conclusions

In the present study, the sound generation mechanisms during the interactions of two vortices at low Mach number are investigated theoretically and numerically. The method of contour dynamics is used for the computation of the motions of the vortex boundaries, while the sound source strengths are calculated based on the vortex sound theory. The vortex systems concerned are the two-dimensional vortices, vortex pairs and vortex rings. Leapfrogging, collision and coalescence interactions are investigated.

For all the vortex systems with small core deformations, it is found that the core deformation produces high-frequency source strength fluctuations. The vorticity centroid dynamics generate relatively low-frequency source strength fluctuations. However, owing to the effect of the core deformation on the vorticity centroid dynamics, there are high-frequency components embedded in these low-frequency fluctuations. The frequency of the high-frequency source strength fluctuations produced by a vortex or a vortex ring is proportional to the strength of the vortex/vortex ring concerned. Since the high-frequency farfield pressure fluctuations increase the sound power radiated significantly, the sound effectively produced by the vortex core deformation, therefore, heavily depends on the circulation of each interacting vortex.

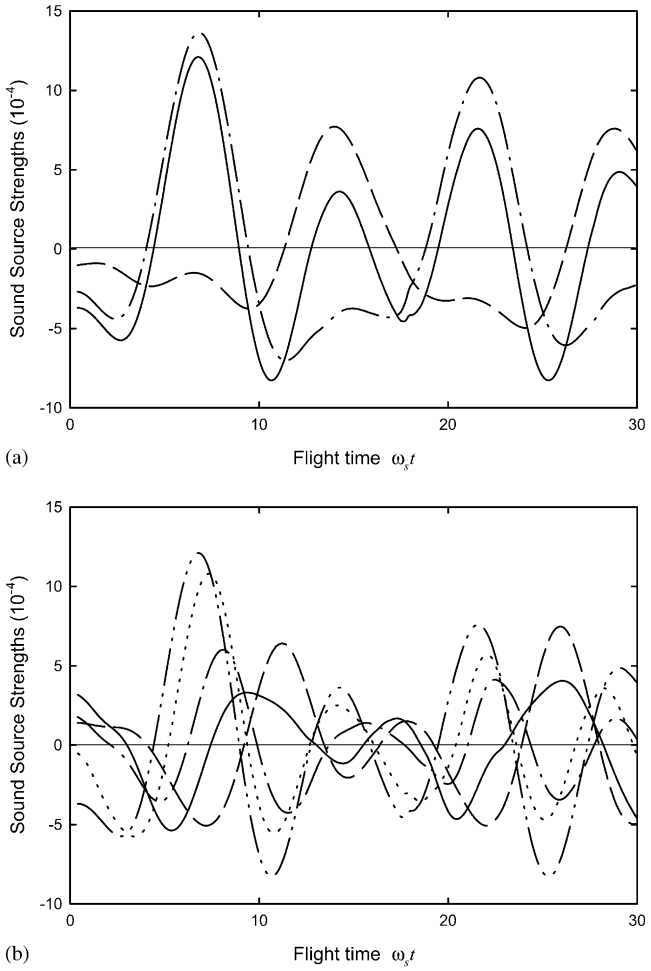

Fig. 20. Sound source strength fluctuations of vortex ring coalescence. $G/R = 0.5$, $\omega_w/\omega_s = 0.866$, $\beta = 0.2$. (a) Contributions from vorticity centroid dynamics and (b) contributions from unsteady core deformation. Legends: same as those in Fig. 17.

When the core deformation becomes serious, the unsteady core deformation dominates the sound generation for the two-dimensional vortex and vortex pair interactions, while the unsteady vorticity centroid dynamics are more important for the vortex ring interactions. The weaker vortical structure during coalescence is found to be more important in the sound generation process.

The results of the present study are summarized in Table 1. They show clearly that the sound produced by simple vortex interactions at low Mach number, independent of the system being two-dimensional or axisymmetrical, moving with steady or unsteady speed and the degree of core deformation, is generated by two basic mechanisms. The first one is the macroscopic vorticity centroid dynamics and the second one the microscopic vortex core fluid motions relative to the vorticity centroid. The latter is related to the deformation of the vortex core from its equilibrium

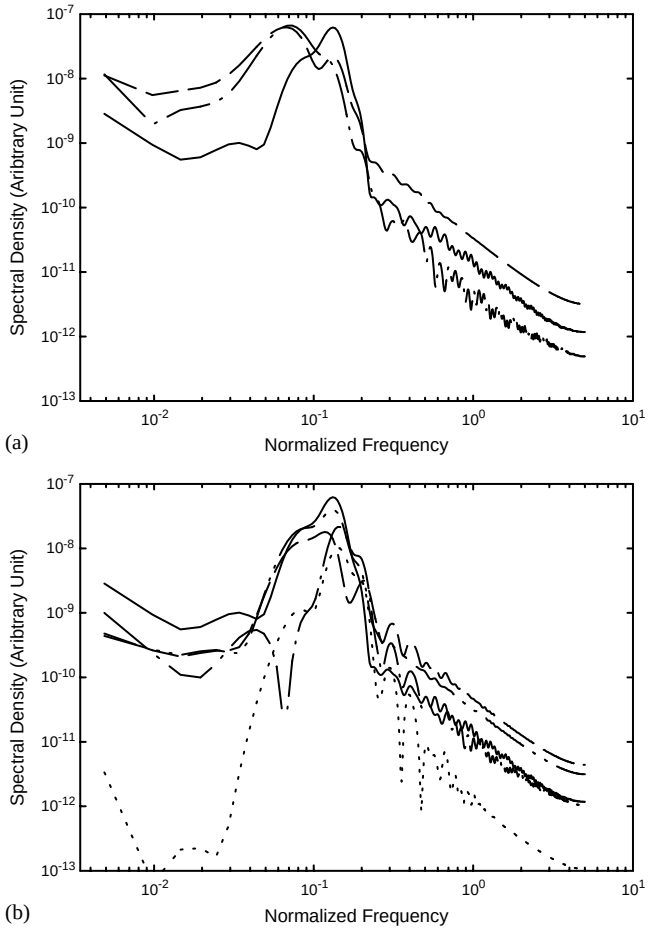

Fig. 21. Frequency characteristics of source strengths of vortex ring coalescence. $G/R = 0.5$, $\omega_w/\omega_s = 0.866$, $\beta = 0.2$. (a) Contributions from vorticity centroid dynamics. (—) Total contribution from vorticity centroid dynamics; (— · —) contribution from stronger vortex ring; (— —) contribution from weaker vortex ring. (b) Contributions from unsteady core deformation. (… …) Overall source strength; (—) total contribution from vorticity centroid dynamics; (— · —) total contribution from unsteady core deformation; (— · · —) contribution from core deformation of stronger vortex ring; (— —) contribution from core deformation of weaker vortex ring.

shape and is of higher frequency than that produced by the former mechanism. The present results have, therefore, generalized and further substantiated the previous findings of the authors. Also, they summarize the similarities and differences between the sound generation processes of two-dimensional and axisymmetric vortex systems, which are not presented in existing literature.

However, one should bear in mind that the interactions considered here are simple ones, which may not be representing exactly those that take place inside a real turbulent shear layer. The scales associated with core deformation and centroid movement are also unclear in real scenario. A further study using direct numerical simulation appears to be useful in the topic, especially when the present idea is extended to the aeroacoustics of low-Mach-number turbulent shear flows.

Table 1
Summary of major sound generation mechanisms in different vortex interactions

Interaction	Vortex system	Major mechanisms	Dominating vortex	Remarks
Leapfrogging	Two-dimensional vortices	Both	Both vortices	Core deformation produces high-frequency sound. Stronger vortex has higher contribution Vorticity centroid dynamics gives low-frequency sound. Weaker vortex has higher contribution
	Vortex pairs	Both	Both vortex pairs	Core deformation produces high-frequency sound. Similar contributions from both vortices Vorticity centroid dynamics gives pulses at slip-through instants from the pair whose cores are further away from the y_1-axis.
	Vortex rings	Both	Both vortex rings	Core deformation produces high-frequency sound. Similar contributions from both rings; Vorticity centroid dynamics gives pulses at slip-through instants from the ring with larger instantaneous radius.
Collision	Vortex pairs	Both	Both vortex pairs	High-frequency sound comes from core deformation. Stronger ring has higher contribution Slowly varying source strength is due to vortcity centroid dynamics of both vortex pairs
	Vortex rings	Both	Both vortex rings	High-frequency sound comes from core deformation. Stronger ring has higher contribution Large pulse at slip-through instant is due to the vortcity centroid dynamics of weaker ring.
Coalescence	Two-dimensional vortices	Core deformation	Weaker vortex	Two sound generation mechanisms tend to counteract each other Effect of vorticity centroid dynamics on sound generation vanishes
	Vortex pairs	Core deformation	Weaker vortex pair	Same as those for the case of two-dimensional vortex coalescence
	Vortex rings	Vorticity centroid dynamics	Both vortex rings	Two sound generation mechanisms tend to counteract each other Effect of core deformation on sound generation vanishes Weaker ring is slightly more important

Acknowledgements

The financial supports from the Haking Wong donation and the Research Grant Council of the HKSAR Government are gratefully acknowledged.

Appendix A. Two-dimensional vortex sound field

The result of Möhring [11] suggests that the farfield pressure fluctuations due to two-dimensional unsteady vortex motions can be found using the formula

$$p(\boldsymbol{x},\tau)=\frac{\rho}{4\pi c}\frac{\partial^3}{\partial\tau^3}\int_{-\infty}^{\tau-|x|/c}\oint\frac{(\hat{\boldsymbol{x}}\cdot\boldsymbol{y})\boldsymbol{y}\cdot(\omega\times\hat{\boldsymbol{x}})}{\sqrt{c^2(\tau-t')^2-|\boldsymbol{x}|^2}}\,\mathrm{d}y_1\,\mathrm{d}y_2\,\mathrm{d}t', \tag{A.1}$$

where the product $(\hat{\boldsymbol{x}}\cdot\boldsymbol{y})\boldsymbol{y}\cdot(\omega\times\hat{\boldsymbol{x}})$ is evaluated at time t' and use has been made of $|\boldsymbol{x}|\gg|\boldsymbol{y}|$. The wavelength of the sound generated is assumed to be much larger than the vortex core dimension. With loss of generality, let $\boldsymbol{x}=x_1\hat{y}_1+x_2\hat{y}_2$ and $\boldsymbol{y}=y_1\hat{y}_1+y_2\hat{y}_2$. One finds,

$$\oint\frac{(\hat{\boldsymbol{x}}\cdot\boldsymbol{y})\boldsymbol{y}\cdot(\omega\times\hat{\boldsymbol{x}})}{\sqrt{c^2(\tau-t')^2-|x|^2}}\,\mathrm{d}y_1\,\mathrm{d}y_2=\frac{1}{\sqrt{c^2(\tau-t')^2-|\boldsymbol{x}|^2}}\times\left(\cos 2\theta\oint\omega y_1y_2\,\mathrm{d}A+\sin 2\theta\oint\frac{y_2^2-y_1^2}{2}\omega\,\mathrm{d}A\right). \tag{A.2}$$

The time integration involved in Eq. (A.1) can be transformed into a line integration in the y_3 direction from $-\infty$ to $+\infty$ by observing that $t'=\tau-|\boldsymbol{x}-y_3\hat{y}_3|/c$ as mentioned in [13] and derived in Ffowcs Williams and Hawkings [36]. Some details on this transformation can also be found in Tang and Ffowcs Williams [37]. Eq. (A.1) becomes

$$p(\boldsymbol{x},\tau)=\frac{\rho_0}{8\pi c^2}\int_{-\infty}^{\infty}\frac{1}{|\boldsymbol{x}-y_3\hat{y}_3|}\frac{\partial^3}{\partial t^3}\left(\cos 2\theta\oint\omega y_1y_2\,\mathrm{d}A+\sin 2\theta\oint\frac{y_2^2-y_1^2}{2}\omega\,\mathrm{d}A\right)\mathrm{d}y_3. \tag{A.3}$$

where the differentiation is done at the retarded time $\tau-|\boldsymbol{x}-y_3\hat{y}_3|/c$. Since $|\boldsymbol{x}|\gg|\boldsymbol{y}|$, Eq. (A.3) can be approximated by Eq. (4) if one includes y_3 into $\boldsymbol{y}$. Though the sound radiated out from various parts along the y_3 direction of the two-dimensional source arrives at $\boldsymbol{x}$ at different time, the source strengths can still be described by $\partial^3/\partial t^3\oint\omega y_1y_2\,\mathrm{d}A$ and $\partial^3/\partial t^3\oint(y_2^2-y_1^2/2)\omega\,\mathrm{d}A$. A Fourier transform of Eq. (A.3) with respect to τ, after transforming the integral along y_3 back into a time integral, gives the formula used by Knio et al. [9] when $|k\boldsymbol{x}|\to\infty$, where k is the wave number of the sound generated. One can also observe that the source term in the formula of Knio et al. [9] is the Fourier Transformed form of the present source terms in Eq. (A.3).

References

[1] M.J. Lighthill, On sound generated aerodynamically I. General theory, Proceedings of the Royal Society of London, Series A 211 (1952) 564–587.
[2] A. Powell, Vortex sound theory, Journal of the Acoustical Society of America 36 (1964) 177–195.

[3] J.E. Ffowcs Williams, A.J. Kempton, The noise from the large-scale structure of a jet, Journal of Fluid Mechanics 84 (1978) 673–694.
[4] P.E. Doak, Fluctuating total enthalpy as the basic generalized acoustic field, Theoretical and Computational Fluid Dynamics 10 (1998) 115–133.
[5] T. Colonius, S.K. Lele, P. Moin, Sound generation in a mixing layer, Journal of Fluid Mechanics 330 (1997) 375–409.
[6] B.E. Mitchell, S.K. Lele, P. Moin, Direct computation of the sound generated by vortex pairing in an axisymmetric jet, Journal of Fluid Mechanics 383 (1999) 113–142.
[7] J.B. Freund, Noise sources in a low-Reynolds-number turbulent jet at Mach 0.9, Journal of Fluid Mechanics 438 (2001) 277–305.
[8] D. Küchemann, Report on the I.U.T.A.M. Symposium on concentrated vortex motions in fluids, Journal of Fluid Mechanics 21 (1965) 1–20.
[9] O.M. Knio, L. Collorec, D. Juvé, Numerical study of sound emission by 2D regular and chaotic vortex configurations, Journal of Computational Physics 116 (1995) 226–246.
[10] W. Möhring, On vortex sound at low Mach number, Journal of Fluid Mechanics 85 (1978) 685–691.
[11] W. Möhring, Modelling low Mach number noise, in: E.-A. Müller (Ed.), Mechanics of Sound Generation in Flows, Springer, Berlin, 1979.
[12] M.S. Howe, Contributions to the theory of aerodynamic sound, with application to excess jet noise and the theory of the flute, Journal of Fluid Mechanics 71 (1975) 625–673.
[13] S.K. Tang, N.W.M. Ko, Sound generation by interaction of two inviscid two-dimensional vortices, Journal of the Acoustical Society of America 102 (1997) 1463–1473.
[14] R.C.K. Leung, S.K. Tang, I.C.K. Ho, N.W.M. Ko, Vortex pairing as a model for jet noise generation, American Institute of Aeronautics and Astronautics Journal 34 (1996) 669–675.
[15] S.K. Tang, N.W.M. Ko, On sound generated by the interaction of two inviscid vortex rings moving in the same direction, Journal of Sound and Vibration 187 (1996) 287–310.
[16] S.K. Tang, N.W.M. Ko, Sound generation by a vortex ring collision, Journal of the Acoustical Society of America 98 (1995) 3418–3427.
[17] S.K. Tang, N.W.M. Ko, A study on the noise generation mechanism in a circular jet, Transactions of the American Society of Mechanical Engineers: Journal of Fluids Engineering 115 (1993) 425–435.
[18] S.K. Tang, N.W.M. Ko, Sound sources in the interactions of two inviscid two-dimensional vortex pairs, Journal of Fluid Mechanics 419 (2000) 177–201.
[19] A.K.M.F. Hussian, K.B.M.Q. Zaman, Vortex pairing in a circular jet under controlled excitation. Part 2. Coherent structure dynamics, Journal of Fluid Mechanics 101 (1980) 493–544.
[20] N.J. Zabusky, M.H. Hughes, K.V. Roberts, Contour dynamics for the Euler equations in two dimensions, Journal of Computational Physics 30 (1979) 96–106.
[21] C. Pozrikidis, The nonlinear instability of Hill's vortex, Journal of Fluid Mechanics 168 (1986) 337–367.
[22] C. Pozrikidis, J.J.L. Higdon, Nonlinear Kelvin–Helmholtz instability of a finite vortex layer, Journal of Fluid Mechanics 157 (1985) 225–263.
[23] S.C. Crow, Aerodynamic sound emission as a singular perturbation problem, Studies in Applied Mathematics 49 (1970) 21–44.
[24] H. Lamb, Hydrodynamics, Cambridge University Press, Cambridge, 1993.
[25] J. Norbury, A family of steady vortex rings, Journal of Fluid Mechanics 57 (1973) 417–431.
[26] R.T. Pierrehumbert, A family of steady translating vortex pairs with distributed vorticity, Journal of Fluid Mechanics 99 (1980) 129–144.
[27] C.D. Winant, F.K. Browand, Vortex pairing, the mechanism of turbulent mixing layer growth at moderate Reynolds number, Journal of Fluid Mechanics 63 (1974) 237–255.
[28] A.E.H. Love, On the motion of paired vortices with a common axis, Proceedings of the London Mathematical Society 25 (1894) 185–194.
[29] H. Yamada, T. Matsui, Mutual slip-through of a pair of vortex rings, Physics of Fluids 22 (1979) 1245–1249.
[30] F.W. Dyson, The potential of an anchor ring—Part II, Philosophical Transactions of the Royal Society of London, Series A 184 (1893) 1041–1106.

[31] C.W. Ng, V.S.Y. Cheng, N.W.M. Ko, Numerical study of vortex interactions behind two circular cylinders in bistable flow regime, Fluid Dynamics Research 19 (1997) 379–409.
[32] S.K. Tang, N.W.M. Ko, Coherent structure interactions in an unexcited coaxial jet, Experiments in Fluids 17 (1994) 147–157.
[33] T. Kambe, T. Minota, Acoustic wave radiated by head-on collision of two vortex rings, Proceedings of the Royal Society of London, Series A 386 (1983) 277–308.
[34] K. Shariff, A. Leonard, N.J. Zabusky, J.H. Ferziger, Acoustics and dynamics of coaxial interacting vortex rings, Fluid Dynamics Research 3 (1988) 337–343.
[35] P.A. Jacobs, D.I. Pullin, Coalescence of stretching vortices, Physics of Fluids 28 (1985) 1619–1625.
[36] J.E. Ffowcs Williams, D.L. Hawkings, Shallow water wave generation by unsteady flow, Journal of Fluid Mechanics 31 (1968) 779–788.
[37] S.K. Tang, J.E. Ffowcs Williams, Acoustic radiation of a vortex approaching a circular cylinder with surface suction, Acoustica 84 (1998) 1007–1013.